Paper pa02-067
Submitted to the 28th International Conference on High Energy Physics
ICHEP'96, Warsaw, Poland, July 1996

Inclusive Diffractive Invariant Mass Distributions in Photoproduction at HERA.

H1 Collaboration

Abstract

The differential cross-section, $\frac{d\sigma^D}{dM_X^2}$, for diffractive photoproduction processes in which the proton remains intact and a system of mass M_X is produced at the photon vertex is presented at an average γp centre of mass energy, $\langle W \rangle = 187$ GeV. It is found to display an elastic peak and a higher mass continuum consistent with Regge predictions based on a triple pomeron amplitude. The differential cross-section is unfolded to obtain separate total cross-sections for elastic and dissociative processes.

1 Introduction

Diffraction dissociation in the real γp system has been the subject of previous study at comparatively small centre of mass energy [1], and has corroborated the Vector Dominance model [2] picture of the high energy photon as behaving in a manner typical of hadrons. Samples of events containing tagged final state electrons scattered at very small angles to the beam are used by the HERA experiments to infer cross-sections in the γp system by means of the Weizsäcker-Williams approximation [3] for the photon flux. Results from HERA on the total γp cross-section [4, 5] and exclusive light vector meson photoproduction [6, 7] have been well described in the Regge picture in terms of a single pomeron trajectory, consistent with that obtained by Donnachie and Landshoff in fits to pp and $\bar{p}p$ total cross-sections [8]. Estimates of cross-sections for photoproduction processes involving diffraction dissociation have previously been made at HERA [4, 5] and indicate that approximately 45% of the total γp cross-section is diffractive in one form or another.

The results presented here are based on two short (~ 25 nb^{-1}) runs in 1994 when HERA was colliding positrons at 27.5 GeV with protons at 820 GeV and minimally biased photoproduction triggers were activated. In one of the runs the event vertex was in the usual position relative to H1 and in the other it was shifted by 70 cm in the forward direction [1], enhancing the detection efficiency for photon fragments. Inclusive cross-sections for diffractive processes are obtained at a γp centre of mass energy averaged over the photon flux of $\langle W \rangle = 187$ GeV.

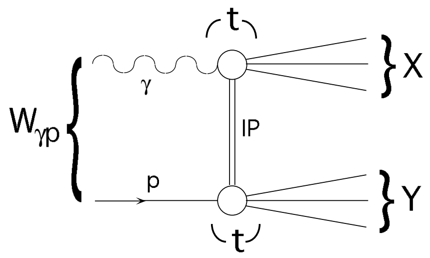

Figure 1: Schematic illustration of the process, $\gamma p \to XY$, showing the kinematic variables discussed in the text.

Four distinct diffractive processes are distinguished, all of which proceed via a colourless exchange generically termed a pomeron ($I\!P$), and each of which in general yields a large gap in the rapidity distribution of final state hadrons between the photon and proton fragmentation regions. All four processes can be discussed in terms of the generalised diagram shown in figure 1. The first *quasi-elastic* case, $\gamma p \to Vp$, corresponds to the situation in figure 1 where the system X consists of one of the lowest lying vector meson states, $V = \rho^0, \omega, \phi$ and the system Y is a leading proton. The second process is *single photon dissociation*, $\gamma p \to Xp$, in which the proton remains intact and the photon dissociates to a continuum of states with mass, M_X. In the third case, *single proton dissociation*, $\gamma p \to VY$, a vector meson is produced at the photon vertex, and the proton dissociates to a system of mass, M_Y. Finally, in the case of *double dissociation*, $\gamma p \to XY$, both of the interacting particles dissociate.

[1]The forward direction is defined to be that of the outgoing proton beam.

With q and P denoting the 4-vectors of the incoming photon and the proton respectively and X and Y denoting 4-vectors for the two distinct components of the hadronic final state, the usual kinematic variables are defined

$$t = (P - Y)^2 \qquad\qquad s = W^2 = (q + P)^2$$

2 Experimental Method

This analysis is concerned with the measurement of diffractive processes in which the proton survives the interaction. The trigger used is based on a combination of a signal from the electron tagger of the H1 luminosity system (eTag) [9] and the detection of activity that is "in time" with a HERA bunch crossing in the twin plastic scintillator walls of the Time of Flight (ToF) device. The backward location of this detector component ($-3.5 < \eta < -2.0$) [2] provides high triggering efficiency at all values of M_X. Badly reconstructed electrons are removed from the sample by placing a fiducial cut on the location of the electron cluster in the eTag, and Bremsstrahlung background is suppressed by demanding no activity above threshold in the Photon Detector of the luminosity system. The principal background to the samples then arises from electron interactions with residual gas particles in the beam-pipe. This is reduced with cuts on the total energy reconstructed in the calorimeters. Since dissociation processes at low M_X do not often give reconstructed tracks in the central parts of the detector, events in which no vertex is reconstructed are retained. However, any event in which a vertex is reconstructed more than 3σ from the nominal interaction point is rejected. Residual beam-gas background is subtracted statistically using the rates obtained from non-interacting electron pilot bunches.

The experimental selection of diffractive events with a leading proton is based on the presence of a rapidity gap spanning at least the laboratory range, $3.0 < \eta < 7.0$, inferred from the absence of activity in the Proton Remnant Tagger, Forward Muon Detector and the more forward part of the Liquid Argon Calorimeter [9]. The system, X, is then taken to be composed of all particles produced backward of the gap. The lower limit of 7.0 on the rapidity reached by the fragments of Y restricts its mass to $M_Y \lesssim 1.6$ GeV. In this region, Monte Carlo studies [10, 11] indicate that there is a small ($\sim 7\%$) contamination with diffractive events that are inelastic at the proton vertex, and an appropriate correction is made.

In order to reconstruct the mass, M_X, a mixed method has been devised [12] which uses Backward Electromagnetic Calorimeter (BEMC) [9], Liquid Argon Calorimeter and tracking information, whilst avoiding double counting. The requirement that no activity be detected forward of $\eta = 3$ ensures that X is well contained in the forward direction. However, losses in the backward direction do occur, both into the beam-pipe and because of the poor containment of hadrons by the BEMC. In order to minimise the effect of such losses, the mass of the system X is reconstructed from

$$M_X = \sqrt{2E_\gamma \, (E + p_z)_X + Q^2 + t}$$

[2] Laboratory pseudorapidity, $\eta = -\ln\tan\frac{\theta}{2}$, is positive in the forward (proton) direction.

where E_γ is the energy of the interacting photon in the laboratory, inferred from the scattered electron energy measurement. $(E + p_z)_X$ is obtained from the reconstructed hadrons and has the property of being insensitive to very backward going particles with $E \simeq -p_z$ that are typically not detected. Since the experimental resolution on t and Q^2 is much greater than their mean values in the sample, both are assumed to be zero.

3 Results

Figure 2a shows the comparison between reconstructed and generated masses in simulations of diffractive events based on the PYTHIA [11] Monte Carlo. Good reconstruction is obtained for all masses, including those consistent with exclusive vector meson production. Figure 2b shows the correlation for the full minimum bias nominal vertex data sample before diffractive cuts, between the reconstructed value of M_X and the maximum pseudorapidity, $\eta_{\max}$, reached by the detected fragments of X. The data at large $\eta_{\max}$ are dominated by non-diffractive processes in which there is no clear rapidity gap and $\eta_{\max}$ is near to the limit of the acceptance of the Liquid Argon calorimeter. Vector mesons and low mass dissociation states appear at very small values of $\eta_{\max}$, where a dependence of the form $\eta_{\max} \sim \ln M_X$ is superimposed, expected when the system X decays on average in an isotropic manner. A clear change in the dynamics of the photon dissociation process is observed in the region of $M_X^2 \sim 5$ GeV^2, above which a correlation of the form $\eta_{\max} \sim \ln M_X^2$ is shown. Such a behaviour is expected in models [13] in which the final state hadron distribution is limited in p_T. Figures 2c and 2d show uncorrected mass distributions obtained in the two samples after application of the cuts based on the forward detector components, compared to an average of the predictions of the PYTHIA [11] and PHOJET [10] models of soft photoproduction. An elastic peak is observed in both samples, along with a higher mass continuum that extends until the system X reaches the limit set by the cut at $\eta_{\max} = 3.0$.

The differential cross-section, $\frac{d\sigma^D}{dM_X^2}$, for all diffractive processes that are elastic at the proton vertex is obtained by correcting the data for detector inefficiency and smearing using simulations based on the Monte Carlo models. Since the two models describe the data equally well, an average is used to make the correction. Results from the nominal and shifted vertex data samples are combined and the final cross-section measurement is shown in figure 3.

In the "triple Regge" region ($M_X^2 \to \infty$, $W^2/M_X^2 \to \infty$), the dynamics of dissociation processes have been shown [14] to be well described via Mueller's optical theorem [15] by combinations of triple Regge amplitudes, which at low values of M_X^2/W^2 are dominated by the triple pomeron amplitude [16]. In the measured region, the minimum kinematically permissible value of $|t|$ is close to zero. Assuming that the triple pomeron diagram dominates and parameterising the product of the triple pomeron coupling and the couplings of the pomeron to external particles by $e^{b_0 t}$, the differential cross-section is expected to behave at fixed W as [17]

$$\frac{d\sigma^D}{dM_X^2} \sim \left(\frac{1}{M_X^2}\right)^{\alpha(0)} \cdot \left(b_0 + 2\alpha' \ \ln \frac{W^2}{M_X^2}\right)^{-1} \tag{1}$$

where $\alpha(t) = \alpha(0) + \alpha' t$ is the pomeron trajectory, and the second term arises from integration over t. At sufficiently large M_X, a fit to the form, $\frac{d\sigma^D}{dM_X^2} \sim (1/M_X^2)^n$ is shown in figure 3. The result is $n = 1.03 \pm 0.02(\mathrm{stat.}) \pm 0.07(\mathrm{syst.})$, illustrating that the data display the approximate $1/M_X^2$ dependence characteristic of diffractive dissociation. A fit to the full form of equation 1 yields $\alpha(0) = 1.11 \pm 0.02(\mathrm{stat.}) \pm 0.07(\mathrm{syst.})$, where we have taken $\alpha' = 0.25$ GeV^{-2} and $b_0 = 3 \pm 1$ GeV^{-2}, estimated from fixed target data [1]. The proximity of the extracted $\alpha(0)$ to the established value of 1.08 [8] confirms that the dominant contribution to the cross-section for the dissociation of photons to low mass states arises from the triple pomeron amplitude.

The Monte Carlo models are used to unfold the points in figure 3 to total cross-sections for elastic and dissociative processes at $\langle W \rangle = 187$ GeV. We obtain $\sigma(\gamma p \rightarrow Vp) = 18.2 \pm 0.8(\mathrm{stat.}) \pm 2.8(\mathrm{syst.})$ μb where $V = \rho^0$, ω or ϕ, and $\sigma(\gamma p \rightarrow Xp) = 21.5 \pm 0.6(\mathrm{stat.}) \pm 5.9(\mathrm{syst.})$ μb for dissociative processes with $M_X^2/W^2 < 0.05$. These measurements confirm our previous results on the decomposition of the total γp cross-section [4] and uncertainties are reduced.

4 Summary and Conclusions

An analysis has been presented of diffractive photoproduction processes at HERA and the invariant mass distribution of the component of the final state produced at the photon vertex studied. This distribution has been shown to correlate with the limiting rapidity reached by the photon fragments in the manner expected for soft hadron-hadron interactions. A sample of diffractive events in which the proton dominantly remains intact has been isolated and used to measure the elastic and single photon dissociation differential cross-section, $\frac{d\sigma^D}{dM_X^2}$. This cross-section displays a peak in the region of the light vector mesons, ρ, ω and ϕ and a dissociation continuum at larger masses. In the triple Regge region, the differential cross-section is in good agreement with a prediction based on the triple pomeron amplitude.

Acknowledgements

We are grateful to the HERA machine group whose outstanding efforts have made and continue to make this experiment possible. We thank the engineers and technicians for their work in constructing and now maintaining the H1 detector, our funding agencies for financial support, the DESY technical staff for continual assistance, and the DESY directorate for the hospitality which they extend to the non–DESY members of the collaboration.

References

[1] T. Chapin et al., Phys. Rev. **D31** (1985) 17.

[2] J.J. Sakurai, Ann. Phys. **11** (1960) 1.

[3] C. Weizsäcker, Z. Phys. **88** (1934) 612.
E. Williams, Phys. Rev. **45** (1934) 729.
S. Frixione et al., Phys. Lett. **B319** (1993) 339.

[4] H1 Collaboration, S. Aid et al., Z. Phys. **C69** (1995) 27.

[5] ZEUS Collaboration, M. Derrick et al., Z. Phys. **C63** (1994) 391.

[6] ZEUS Collaboration, M. Derrick et al., Z. Phys. **C69** (1995) 39.

[7] H1 Collaboration, I. Abt et al., Nucl. Phys. **B463** (1996) 3.

[8] A. Donnachie, P. Landshoff, Phys. Lett. **B296** (1992) 227.

[9] H1 Collaboration, I. Abt et al., "The H1 Detector at HERA", DESY preprint **93–103** (July 1993).

[10] R. Engel, Proceedings of the XXIXth Rencontre de Moriond (Editions Frontieres, 1994) 231.
R. Engel, Z.Phys. **C66** (1995) 203.

[11] H. Bengtsson, T. Sjöstrand, Comp. Phys. Commun. **46** (1987) 43.
H. Bengtsson, T. Sjöstrand, Comp. Phys. Commun. **82** (1994) 74.

[12] P. Newman, "A Study of the Dynamics of Diffractive Photoproduction at HERA", PhD Thesis, University of Birmingham (February 1996), RAL-TH-96-011.

[13] D. Amati, A. Stranghellini, S. Fubini, Nuovo Cimento **26** (1962) 896.

[14] For a review, see K. Goulianos, Phys. Rep. **101** (1983) 169.

[15] A. Mueller, Phys. Rev. **D2** (1970) 2963.

[16] D. Roy and R. Roberts, Nucl. Phys. **B 77** (1974) 240.

[17] See for example P. Collins, "An Introduction to Regge Theory & High Energy Physics", Cambridge University Press, Cambridge (1977).

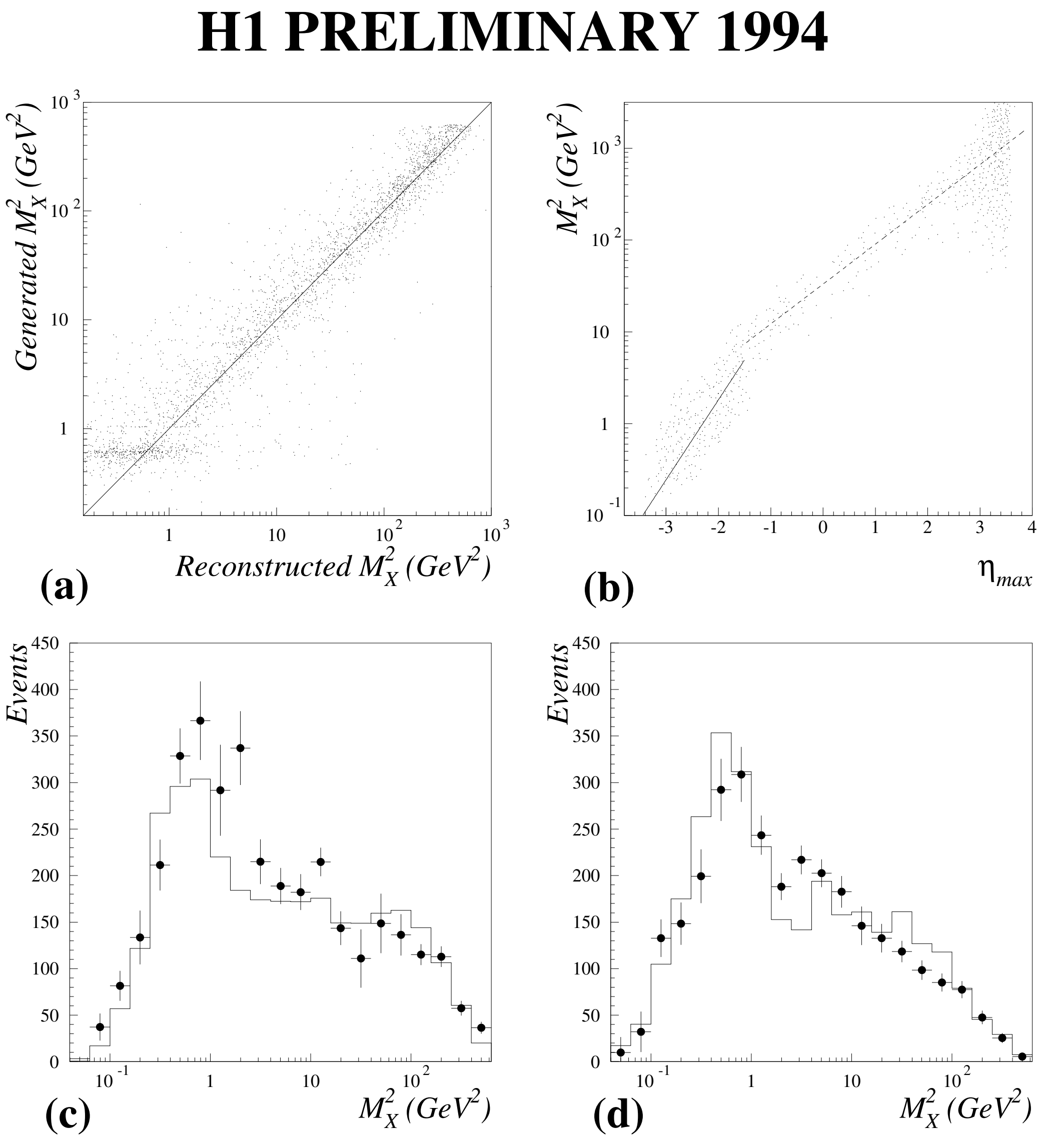

Figure 2: (a) Correlation between reconstructed and generated M_x for diffractive photoproduction events in the PYTHIA Monte Carlo. (b) Correlation between M_x and $\eta_{\max}$ for the full nominal vertex data sample. The superimposed lines are discussed in the text. (c) Uncorrected mass distribution after using the forward detector cuts to obtain a sample of diffractive photoproduction events that are elastic at the proton vertex (nominal vertex sample). The mass spectrum is compared to an average of predictions of two Monte Carlos, normalised through the total γp cross-section. (d) The same plot for the shifted vertex data sample.

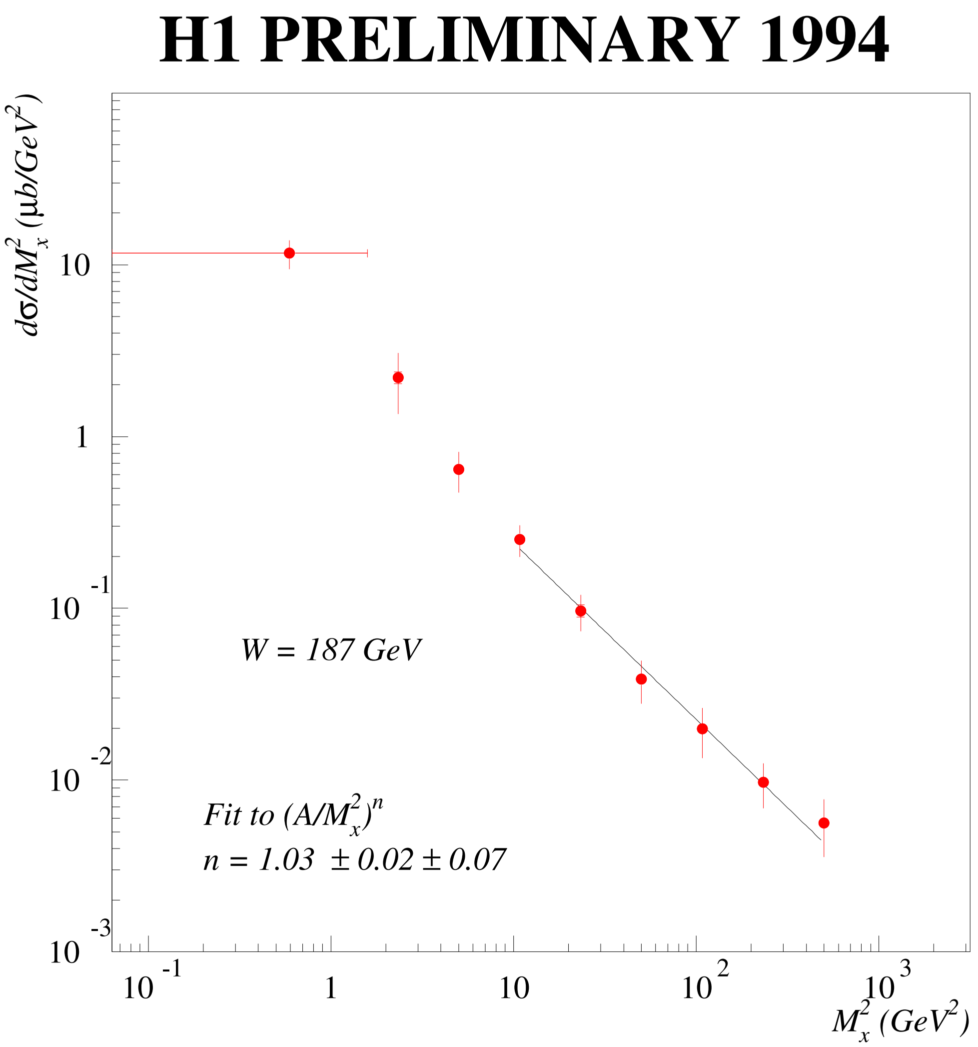

Figure 3: Corrected points obtained for the cross-section $\frac{d\sigma^D}{dM_X^2}$ at $Q^2 = 0$, integrated over t. A fit to the form, $(\frac{1}{M_X^2})^n$ is shown for $10.8 < M_X^2 < 500$ GeV^2.